Parallelized Computational Modeling of Pile-Soil Interactions in Mechanized Tunneling

Günther Meschke, Jelena Ninić, Janosch Stascheit and Abdullah Alsahly

Institute for Structural Mechanics, Ruhr University Bochum, Universitätsstr. 150, 44780 Bochum, Germany

Abstract

The construction of tunnels in soft ground causes short and long term ground deformations resulting from the disturbance of the virgin stress state of the soil and the changing pore water conditions. In particular in urban tunneling, in each stage of the construction process, interactions between the construction process, the soil and existing building infrastructure need to be evaluated to limit the risk of damage on existing buildings and to decide on appropriate mitigation measures. Besides conventional tunneling, mechanized tunneling is a well established and flexible technology in particular in urban areas, which allows for tunnel advances in a wide range of soils and difficult conditions. The paper presents a finite element model for the simulation of interactions between mechanized tunnel construction, the surrounding soil and existing buildings resting on pile foundations in the framework of a process-oriented simulation model for mechanized tunneling. The performance of the model is demonstrated by means of selected prototype analyses. As a consequence of the high computational demand connected with this type of spatio-temporal simulations, problem specific parallelization techniques are investigated to increase the numerical efficiency of the numerical analyses.

Keywords: Finite Element Method, mechanized tunneling, pile foundation, domain decomposition, anchors

1. Introduction

Tunneling in urban environment has become an essential part of infrastructural development worldwide. In this context, the protection of vulnera-

ble buildings from damaging effects of the tunnel construction is a challenge, in particular in soft ground conditions and tunneling with low overburdens. Besides conventional tunneling, mechanized tunneling is a well established and flexible technology in particular in urban areas, which allows for tunnel advances with small cover depths and in different geotechnical conditions including water saturated soft soils. In soft, partially or fully saturated ground conditions, the tunnel construction process causes short and long term ground deformations resulting from the disturbance of the virgin stress state of the soil and the changing pore water conditions. During the construction process in urban tunneling, interactions between the construction process and the environment need to be evaluated to limit the risk of damage on existing buildings and to decide on appropriate mitigation measures. To this end, realistic numerical models able to appropriately consider the interactions between the mechanized tunneling process, the soil and existing surface structures and their foundations during the complete construction process are required. For an adequate representation of the interactions of the tunneling process with the built environment, a number of submodels have to be combined: a realistic model of the tunneling process including the various support methods, a ground model that captures the main characteristics of the ground behavior under tunneling-induced disturbance, and a model for the aboveground structures and their foundations taking into account frictional contact with the ground. In mechanized tunneling, the tunneling process involves various components (the tunnel boring machine (TBM), the soil and groundwater conditions, lining, steering via the hydraulic jacks, tail void grouting and various types of face support) and their relatively complex mutual (time-dependent) interactions. In conventional tunneling by means of the New Austrian Tunneling Method (NATM), besides the staged excavation process, the interactions between the supporting shotctrete shell and grouted anchors and the ground need to be considered.

Although the continuous increase of computing power and the considerable progress in computational modeling have stimulated the development of numerical simulation models in tunneling since the early 1980's, compared to the large number of models developed in the context of NATM tunneling (see, e.g. [1] and references therein), only a limited number of fully three-dimensional numerical models exist for shield tunneling due to its considerably more complex nature, see, e.g. [2, 3, 4, 5]. A prototype for a process-oriented three-dimensional finite element model for simulations of shield-driven tunnels in soft, water-saturated soil has been proposed in

[6] and successfully used for systematic numerical studies of interactions in mechanized tunneling [7]. This model has been recently extended for the process-oriented simulation of shield-driven tunnels in partially saturated soft soils (see, e.g. [8], using a more advanced, flexible software architecture, an automatic model generator [9], a more suitable elasto-plastic model for soft ground conditions [10] and a three-phase model for soft soils to represent face support by means of compressed air in addition to general partially saturated conditions [11]. This model is augmented by components to account for piles embedded in the ground at arbitrary positions and orientations to consider interactions between the tunneling process and existing structures on pile foundations. Here, the interactions between the pile foundation and the surrounding soil is characterized by the coupling of deformations along the interface and at the tip of the pile, and by possible relative slip deformations between the piles and the soil.

Several finite element models have been proposed for the representation of soil-pile interactions. In an early approach by Desai and Appel [12] volume elements for both soil and piles, connected by a thin layer of interface elements have been used. This method, however, requires compatibility of both finite element meshes and hence a rather fine discretization of the soil in the vicinity of the pile. More recent formulations apply surface-to-surface contact conditions [13, 14, 15] or define a void in the soil mesh of the dimensions of the pile that is attached to beam elements by means of node-to-surface contact conditions to account for the soil-pile interactions [16]. Although these approaches do not require compatible discretizations for the piles and the soil, these formulations still require a priori consideration of the location and orientation of the piles in the geometrical setup of the model. An embedded pile formulation proposed by Sadek and Shahrour [17] accounts for piles as beam elements that are discretized independently from the soil. Their interaction with the soil is modeled by detecting intersections of soil and pile elements and inserting interface nodes. Since only one pile may intersect with a finite soil element, the discretization effort is considerable in case of pile groups.

In the paper, a recently developed embedded pile formulation is presented in the context of modeling interactions between the tunneling process and existing buildings resting on pile groups. The pile element allows to consider frictional contact between piles and the soil surface and pile tip resistance along arbitrarily oriented piles embedded within soil elements. As an advantage compared to existing models, the current formulation does not require

the geometry nor the discretization of the soil to be compatible with the layout of the piles. All interaction conditions are enforced in control points of the embedded beam elements forming the piles. The developed embedded pile formulation can also be used to represent rock reinforcement by means of anchors or pipe roofs within the ground surrounding the excavation domain in conventional tunneling [18]. This feature is also addressed in this paper.

To reduce the large computation times connected with the complex process-dependent simulation model, parallelization techniques on shared and distributed memory systems have been developed [19], adopting parallelization strategies to the non-standard finite element technology applied in the simulation model.

The remainder of the paper is organized as follows: Section 2 contains a summary of the main features of the numerical simulation model for shield tunneling employed for the presented analyses. The extension of this model using a frictional embedded pile formulation is described in Section 3. Two numerical examples are presented to demonstrate the capabilities to model the interaction between machine driven tunnel construction underneath a high-rise reinforced concrete building and the use of the embedded pile formulation for modeling rock reinforcement in conventional tunneling. Finally, section 4 addresses parallelization techniques employed to speed up the computation times for the computationally highly demanding simulation model.

2. Computational simulation model for mechanized tunneling

The finite element model for shield driven tunneling developed in the context of an integrated decision support platform (IOPT) for mechanized tunneling has been presented in [20, 21, 11] and is only briefly described here. It has been implemented in the object-oriented finite element framework KRATOS [22] and is denoted as `ekate` (Enhanced Kratos for Advanced Tunneling Engineering). Its main design goal is to provide an efficient yet realistic simulation environment for all interaction processes occurring during machine driven tunnel construction. It includes all relevant components of the mechanized tunneling process as sub-models, representing the partially or fully saturated ground, the tunnel boring machine (TBM), the tunnel lining, hydraulic thrust jacks and the tail void grouting, which are interacting with each other by means of algorithmic coupling. The ground model is formulated within the framework of the theory of porous media (TPM) and accounts for the coupling between the deformations of the solid phase

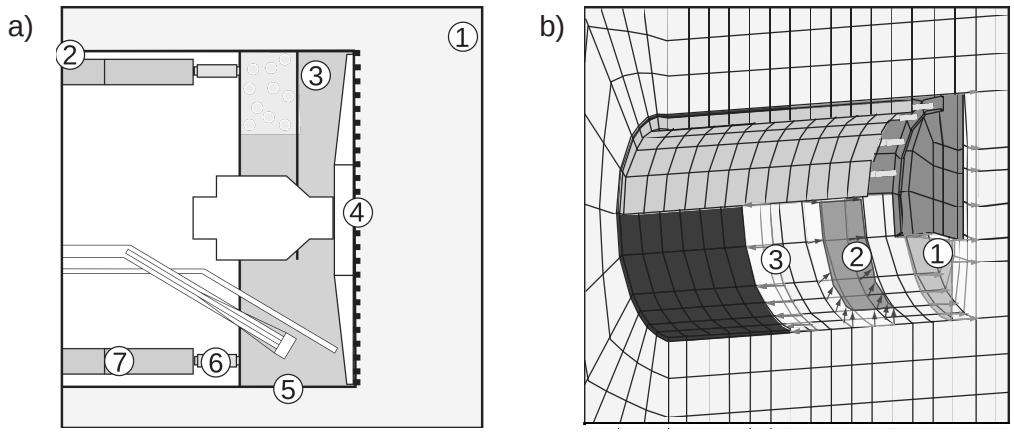

Figure 1: a) Main components involved in mechanized tunneling: (1) soil, (2) tail gap, (3) pressurized support medium, (4) cutting wheel, (5) shield skin, (6) hydraulic jacks and (7) segmented lining. (b) Modeling of interactions between soil and TBM in the simulation model `ekate`: (1) heading face support, (2) frictional contact between shield skin and soil and (3) grouting of the tail gap) and components of the simulation model: TBM (blue), hydraulic jacks (yellow), lining (green) and grouting mortar (purple)

and two fluid pressures (incompressible liquid and compressible air phases) taken as primary variables. Fluid flow through the pores is described using Darcy's law in combination with the concept of relative permeabilities, using the soil-water characteristic curve (SWCC) according to VAN GENUCHTEN. The material behavior of the soil skeleton is modeled by means of a non-linear elasto-plastic constitutive law for clays and sands, proposed in [10]. Quadratic (linear) approximations are used for the approximations of the displacements (pore fluid and air pressures). A detailed description of the multi-phase model for partially saturated soils and its spatial and temporal discretization is given in [23].

Figure 1 shows the main components involved in mechanized tunneling (left) and their representation in the finite element model (right). The TBM is modeled as an independent, deformable body connected along the shield skin to the soil by means of frictional contact conditions; the weight of the structural and machinery parts of the machine are accounted for. The segmented tunnel lining is represented by volume elements that are step-wise activated during the process simulation. The segmentation of the lining is accounted for by means of a homogenized stiffness reduction according to [24]. The lining tube is furthermore used as counter-bearing for the hydraulic jacks

thrusting forward the shield machine. The hydraulic jacks, represented by truss elements take the front surface of the least activated lining segment as the counter-baring for the hydraulic jacks thrusting forward the shield machine by means of prescribed strains induced in the elements. The elongation of each jack element is controlled by a steering algorithm that allows for counter-steering against weight-induced dropping of the TBM to keep the path of the machine on the prescribed tunnel alignment. The simulation of the advancing process for arbitrary alignments requires a continuous adaption of the finite element mesh in the vicinity of the tunnel face in conjunction with the steering algorithm for the TBM advance and appropriate algorithms for the transfer of internal variables. A new technique to automatize the process of mesh generation utilizing a hybrid mesh approach in which a new computational mesh in the vicinity of the tunnel face is automatically generated within the advancing process, is introduced (Figure 2a). To model the pressurized grouting mortar used to fill the gap between lining

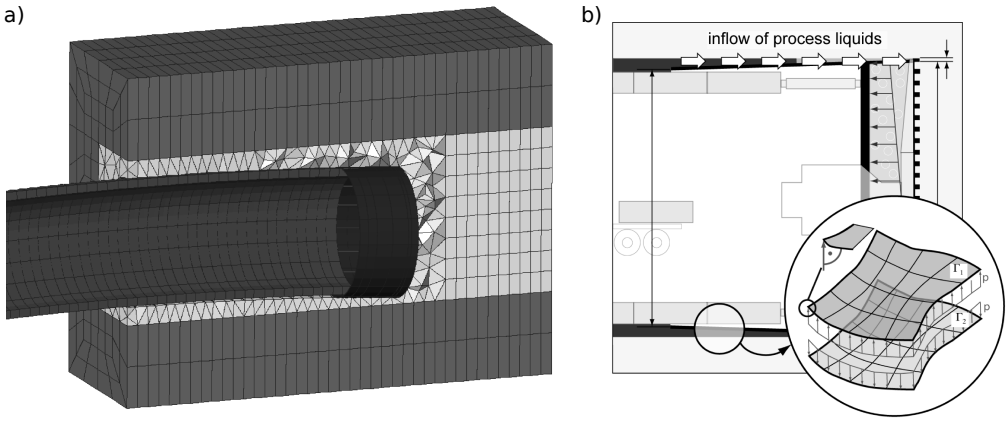

Figure 2: a) Adaptive re-meshing during steering of TBM along curved alignments, b) TBM-soil-interface with flowing-in of process fluids into the steering gap and modeling of the contact between the soil and the shield skin through a surface- based contact formulation with consideration of a pressurized fluid film between the contact surfaces

and ground, a two-phase (hygro-mechanical) formulation similar to the one used for the ground model is applied. Here, the grouting pressure is applied as pore water pressure to the fresh mortar. Stiffening of the grouting mortar is considered while the pore water pressure may dissipate according to an infiltration process into the surrounding ground. The heading face support can be adapted to the requirements posed by the specific TBM. Depending

on the type of face support in hydro- and earth-pressure balance shields the pore water pressure, and the total or effective stresses mechanical pressures or a combination of both can be prescribed. The formation of a filter cake during standstill of the machine can be accounted for by fluctuating application of a combination of mechanical and liquid pressures. Since air pressures in the ground for partially saturated conditions can be prescribed independently, the model also allows to simulate a temporary face support by means of compressed air [25]. Possible flow of process liquids (support fluid and grouting mortar) along the shield skin is considered in the model by means of a finite difference scheme along the element vertices of the shield. A pressurized liquid film between shield and ground is therefore taken into account within the contact formulation [26] (Figure 2b).

3. Embedded finite pile element for modeling of pile-soil interactions

To realistically represent the interactions between the soil and pile foundations in numerical analyses of tunnel advance, an embedded finite element for piles has been developed, which allows to model pile groups independently from the spatial discretization of the soil and accounts for the surface coupling with interface friction between piles and the surrounding soil. In the proposed model piles are represented by means of shear deformable beam elements to account for axial as well as lateral loadings. The spatial discretization of fully (partially) saturated soils is based on two- (three-) phase finite volume elements with quadratic approximations for the displacements and linear approximations for the water (gas) pressure. The beam-soil interaction is formulated in terms of contact conditions, which can be expressed in terms of Kuhn-Tucker optimality conditions characterizing the inequality constraints

$$\begin{aligned} \sigma_N &\geq 0 \\ g &\leq 0 \\ \sigma_N \cdot g &= 0. \end{aligned} \tag{1}$$

In Eq. 1 σ_N denotes the contact stress, and g denotes the gap or penetration between the two bodies, commonly denoted as slave and master elements. In this formulation the beam elements serve as slave elements while the volume elements of the soil are considered as master elements. To this end, each integration point in the pile element is associated with an adjacent target point in the soil element (see Figure 3a). The target point in the soil element

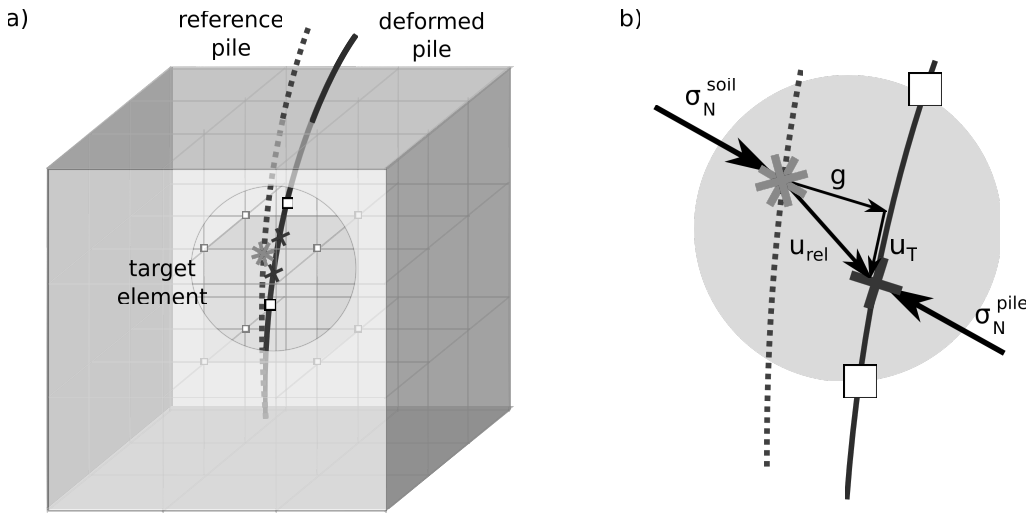

Figure 3: Modeling of pile-soil interaction: a) contact detection strategy: for each integration point of the pile element (cross marks) the target point in the soil element (asterisk marks) with the same global coordinates as the pile integration point is detected; b) definition of gap displacement

is detected using a spatial search that determines the respective volume element (target element) and the local coordinates of a point (target point) within this element that has the same global coordinates as the integration point of the pile element. In this point the interaction conditions stated above are enforced. Since the location of the constraints in the soil elements is independent from the positions of the nodes, this approach allows for a mesh-independent representation of piles and pile groups in an arbitrary soil layout. Frictional response during tangential sliding motions between the pile and the soil is taken into account by means of the COULOMB friction law. To this end, the condition for active frictional response is to be fulfilled in addition to the KUHN-TUCKER conditions (Eq. 1):

$$\begin{aligned} |\sigma_T| &\leq \sigma_N \mu \quad \text{and} \\ \mathbf{u}_T &= \lambda \boldsymbol{\sigma}_T \quad \text{where} \quad \begin{cases} \lambda = 0 & \text{if} \quad |\boldsymbol{\sigma}_T| \leq \sigma_N \mu \\ \lambda \geq 0 & \text{if} \quad |\boldsymbol{\sigma}_T| = \sigma_N \mu \end{cases} \end{aligned} \tag{2}$$

μ denotes the coefficient of friction, $\mathbf{u}_T$ is the tangential motion of a contact point of the pile element relative to the target point in the solid element and $\boldsymbol{\sigma}_T$ is the effective tangential stress in the pile contact point. The friction

model is formulated in analogy to elasto-plastic models, in terms of a slip function Φ, an evolution equation for the plastic slip and loading-unloading conditions [27]:

$$\Phi(\sigma_T, \sigma_N) = \|\sigma_T\| - \sigma_N \mu$$

$$\dot{\mathbf{u}}_T = \dot{\gamma} \frac{\boldsymbol{\sigma}_T}{\|\boldsymbol{\sigma}_T\|} \leq 0, \tag{3}$$

$$\dot{\Phi} \geq 0, \quad \dot{\gamma} \leq 0, \quad \dot{\gamma}\, \Phi = 0.$$

In Eq. 3 $\dot{\gamma}$ denotes the rate of the slip flow, analogous to the rate of plastic flow in elasto-plasticity. Eq. $(3)_1$ is a restatement of Eq. $(2)_1$, while the conditions $(3)_{2-3}$ mimic Eq. $(2)_2$ with one important difference: they express the collinearity of the slip displacement $\dot{\mathbf{u}}_T$ and the frictional stress $\boldsymbol{\sigma}_T$ in rate form, effectively changing the frictional law to one of an evolutionary type [28]. For the regularization of COULOMB's friction problem normal and tangential penalty parameters are used. Based upon the governing equations for frictional contact between two deformable bodies (linear momentum balance, geometrical relations, constitutive relations, contact conditions and initial and boundary conditions), the weak form of the large deformation contact problem is obtained:

$$G^{int,ext}(\varphi_t, \delta\varphi) + G^c(\varphi_t, \delta\varphi) = 0\,, \tag{4}$$

Here, the internal and external virtual work $G^{int,ext}$ is augmented by a contribution G^c of the contact contstaint $g = 0$, which is given as

$$G^c(\varphi_t, \delta\varphi) = \int_{\Gamma_c^{(2)}} [\sigma_{N_t} \delta g + \sigma_{T_t} \delta\xi] d\Gamma\,. \tag{5}$$

σ_N and σ_T are normal and tangential stresses and δg and $\delta\xi$ are normal and tangential virtual displacements, respectively. The algorithmic formulation and implementation is characterized by the spatial discretization of the weak form Eq. 5 using quadratic shape functions for displacements of the solid and linear shape functions for the displacements and rotations of the beam element, respectively. A staggered scheme is used for the integration of the frictional evolution equations, characterized by first solving for the trial state and a subsequent return map algorithm [29], as is commonly employed for the integration of elasto-plastic equations. The respective contact tangent stiffness matrix is computed from consistent linearization of Eq. 5.

3.1. Tip Condition

The interaction between the tip of the embedded pile with the soil is described by an additional embedded interface element. In order to prevent the penetration of the tip into the soil, a complete tying of the displacements is imposed using LAGRANGE multipliers:

$$\begin{bmatrix} \mathbf{K}_{soil} & 0 & -1 \\ 0 & \mathbf{K}_{tip} & 1 \\ 1 & -1 & 0 \end{bmatrix} \cdot \begin{bmatrix} \mathbf{u}_{soil} \\ \mathbf{u}_{tip} \\ \lambda \end{bmatrix} = \begin{bmatrix} \mathbf{R}_{soil} \\ \mathbf{R}_{tip} \\ 0 \end{bmatrix} \Rightarrow \Delta\mathbf{u}_{soil} = \Delta\mathbf{u}_{tip} \qquad (6)$$

where K_{soil} and K_{pile} represent the tangent stiffness matrices of the soil and pile elements, respectively, and λ denotes the LAGRANGE multiplier. In the tip condition the same search algorithm as in the previous formulation is used for contact detection, which allows to model the tip of the pile independent from the soil discretization.

3.2. Comparative study of model performance

To demonstrate the performance of the proposed model to represent the behavior of pile foundations under combined loading, a comparative study has been performed. A single pile embedded in a cube of soil is laterally and axially loaded with 10 kN each. To serve as a reference solution, both the soil and the pile have been modeled using solid elements that are in frictional contact using a surface-to-surface contact model. To investigate the convergence of the proposed beam-solid interaction model, a second model using different levels of mesh densities has been generated (see Figs. 5b and c). The reference (solid-solid) model has been discretized by finite tri-linear volume elements using 22,840 degrees of freedom (DOF). For the analyses using the embedded pile model, five different meshes ranging from 258 DOFs to 11,732 DOFs have been used. Table 1 summarizes the number of finite elements used for the soil and the pile, respectively, the total number of DOFs, the computing time and the relative root mean square error (rRMSE), defined as

$$rRMSE = \sqrt{\frac{\sum_{0}^{NN} \left(\frac{\|\mathbf{u^{ss}} - \mathbf{u^{bs}}\|}{\|\mathbf{u^{bs}}\|} \right)^2}{NN}}, \qquad (7)$$

in terms of the pile displacements $\mathbf{u}^{bs}$ as compared to the respective displacements $\mathbf{u}^{ss}$ from the reference solution, normalized by the size of the problem in terms of the number of nodes NN.

Table 1: Comparison of performance of embedded pile formulation using different discretizations

Model	Discretization Soil	Discretization Pile	DOFs	$rRMSE$ [%]	Time [s]
Reference (3D)	686	156	22840	0	301.63
Beam-solid 1	3x3x3	5	285	23,707	0.690
Beam-solid 2	5x5x5	10	621	14,024	0.860
Beam-solid 3	9x9x9	15	2816	4,790	1.679
Beam-solid 4	11x11x11	20	4886	2,773	2,895
Beam-solid 5	15x15x15	35	11732	0,286	8.641

Fig. 5 contains plots showing the convergence behavior of the embedded pile model with respect of the displacement and the rotation of the pile at the surface level versus the total number of degrees of freedom. The maximum displacement and the maximum slope of the pile at different discretizations are compared to a reference solution using a solid-solid contact formulation (as shown in Fig. 4a). The figure shows that the proposed pile model yields

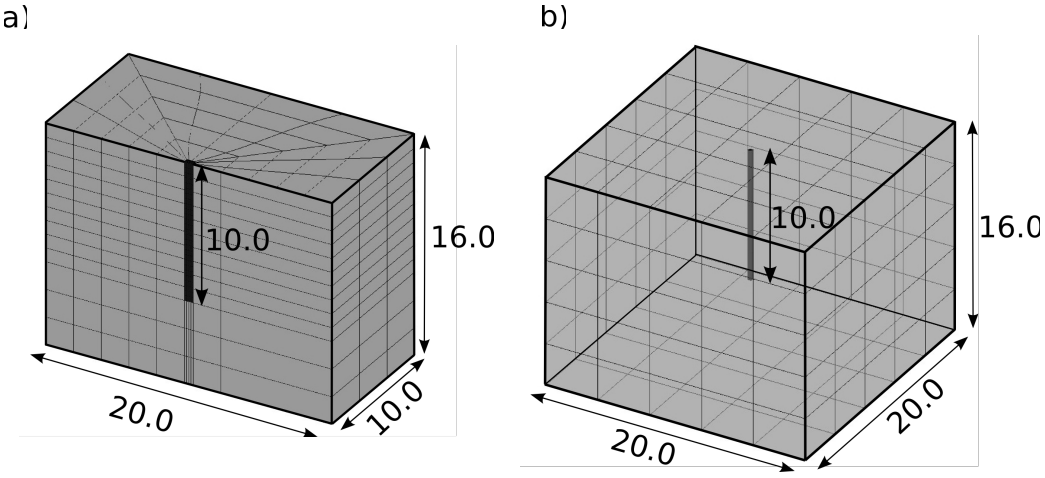

Figure 4: Comparative study of model performance: a) model for reference solution (solid-solid); b) embedded (beam-solid) pile model

results at the same level of accuracy compared to the fully 3D model using less then 50 % of the number of DOFs. Only for a very coarse mesh of the beam-solid model using 3^3 soil elements and 5 beam elements, the solution

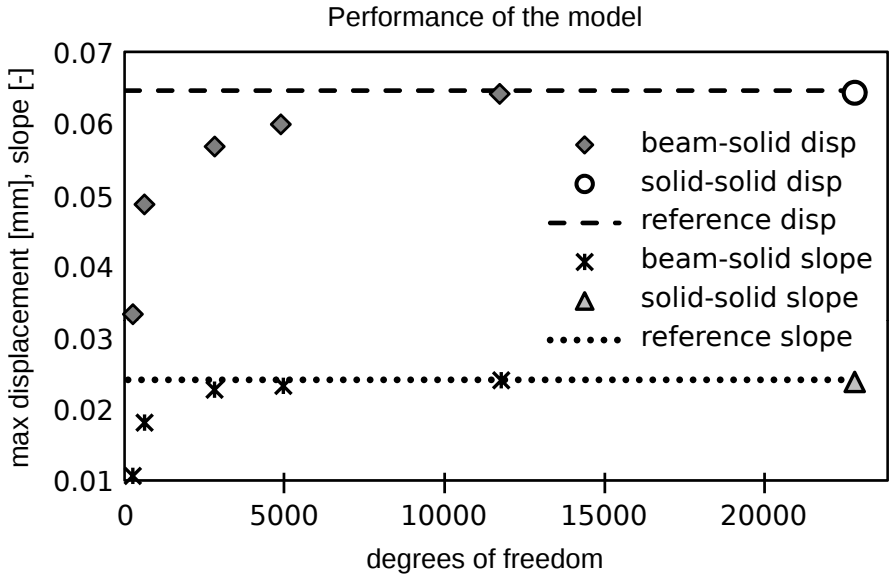

Figure 5: Comparative study of model performance: convergence of solution of the embedded pile (beam-solid) model to a fully 3D (solid-solid) reference solution with respect to the number of degrees of freedom

deviates significantly from the reference solution. With respect to the numerical efficiency it can be noted that the finest model using the embedded pile formulation requires a total computation time of 8.6 seconds compared to the computing time of 301 seconds required for the reference (solid-solid) model.

3.3. Numerical example 1: Analysis of interactions between pile foundations and shield driven tunneling

The pile formulation has been applied for modeling a structural foundation and its interaction with the construction of a tunnel in the vicinity of the building. The model presented in this example is concerned with the construction of a shallow shield driven tunnel in homogeneous, fully saturated soft cohesive soil, symmetrically underneath a building resting upon a group of piles. The purpose of the analysis is to investigate the response of the building and its foundations during the tunnel advancement.

The geometry and the finite element discretization of the computed section of the tunnel drive is presented in Figure 6. For the soil, 9700 3D hexahedral elements with quadratic approximations of the displacements and

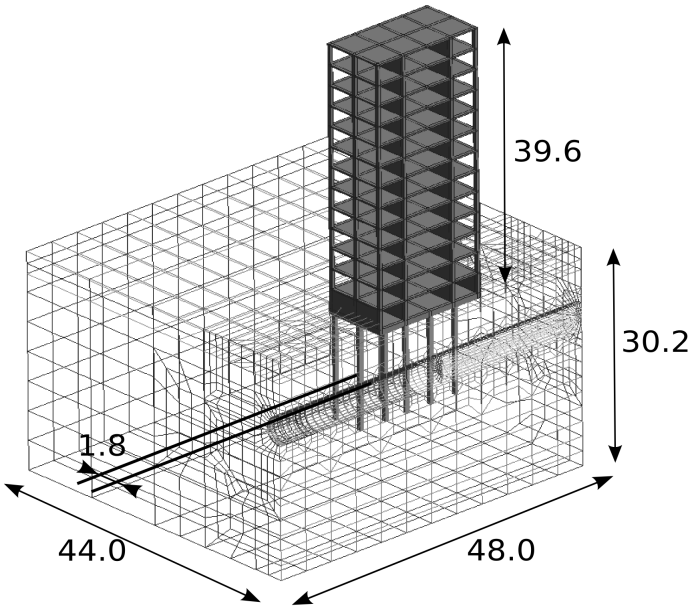

Figure 6: Modeling of TBM driven tunnel construction beneath a high building resting on pile foundation: Geometry and FE discretization (dimensions in [m])

linear approximations for the pore pressure are employed. Each pile is discretized using 15 TIMOSHENKO beam elements. The complete model has 135.069 degrees of freedom. A portion of 48 m of the complete tunneling process is simulated with 48 excavation steps, with a round length of 1 m and assuming an advancement speed of 24 m per day. The excavation diameter D of the tunnel is 4.4 m, the cover depth is 8.17 m. The ground water table is assumed to be at 1.8 m below the ground surface at the level of the building's foundation plate. The soil is represented using a two-phase model for fully saturated soil [11] consisting of a solid phase of the soil skeleton and a fluid phase representing the pore water. The porosity of the soil is assumed as 20 %, and the initial permeability for water and air is assumed as $k_w = 14.4cm/h$ and $k_a = 144.0cm/h$, respectively. For the sake of simplicity and in order to solely capture the interactions between the excavation process and the pile foundations, the solid skeleton of the ground has been modeled using a linear-elastic constitutive model. The ground is assumed to have a Young's modulus of $E = 5.25$ MPa and a Poisson ratio of $\nu = 0.35$. The building is a high-rise residential building, consisting of 12 aboveground

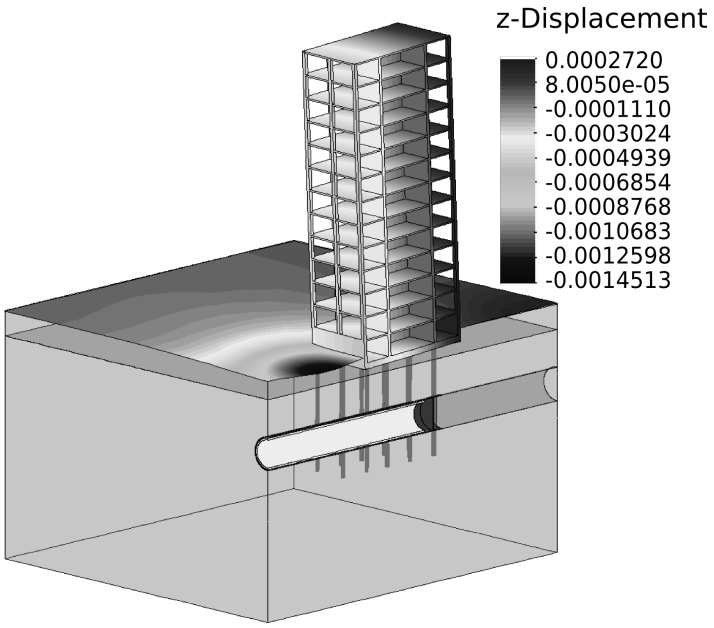

Figure 7: Modeling of TBM driven tunnel construction beneath a high building resting on pile foundation: distribution of vertical displacements at the surface (in [mm]) at a certain stage of the excavation process

levels and one underground level, with based dimensions 16 m x 16 m and a total height of 39.6 m. The building is founded on a group of piles, each 15 m long, with a cross-section of 0.6 m x 0.6 m, uniformly distributed over the foundation plate at relative distances of 4 m each. At the end of each pile the tip condition is applied to simulate impenetrability of the foot of the pile. The tunnel is passing the closest row of piles at a distance of 1.8 m. Both the building and the piles are idealized as linear elastic deformable bodies, with a typical Young's modulus of the concrete of 30 GPa and a specific weight of 25 kN/m^3. Prior to the simulation of the TBM advancement, the in-situ stress state is computed in a separate model that consists of a simple box of undisturbed ground. The initial stress is then applied to the simulation model such that all deformations that are not related to the tunnel excavations are eliminated.

Fig. 7 shows the vertical displacements induced by the tunneling process for the instant when the cutting face of the TBM is passing a control section located along the middle row of the pile group. The influence of the tunnel

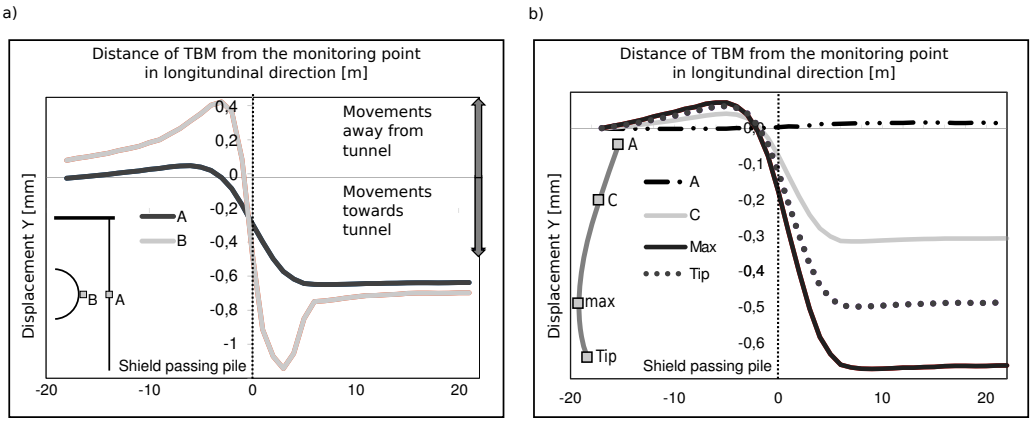

Figure 8: Lateral displacements of piles induced by tuneling process: a) Soil deformations vs. pile deformations; b) horizontal displacement profile of the piles

excavation process on existing piles and the surrounding ground is shown in Figure 8a. In this plot horizontal displacements in two points of the model are compared: one point (A) is located at the point of the innermost pile closest to the excavated tunnel while the other point (B) is located in the soil next to the tunnel lining at a horizontal distance of 1.85 m from the pile. The horizontal displacements are plotted over time while the excavation proceeds. Negative pile displacements indicate movements of the pile towards the tunnel in horizontal direction. It can be observed that, in general, the piles undergo the same evolution of deformations as the surrounding ground with the difference, that the soil displacements exhibit a larger magnitude of deformations. This reflects the stiffening effect of the piles on the structural response of the soil.

The diagram in Figure 8b shows the horizontal displacements of different points distributed over the height of the pile closest to the tunnel plotted over the distance of the tunnel face from the monitoring section. The monitoring section is located at the symmetry plane of the building. The tunnel excavation process induces considerable displacements and curvatures in the pile located at the control section nearest to the tunnel. From the plot it is observed that in the early stages, when the tunnel face is located before the control section, the pile is bending away from the tunnel, due to a high face support pressure. After the tunnel face has passed the location of the pile, the displacements are changing their direction and the pile moves back towards the tunnel as a result of relaxation of stresses.

3.4. Numerical example 2 - Rock reinforcement by grouted anchors in NATM tunneling

In the second example, the proposed embedded finite element model for piles is applied in the context of the New Austrian Tunneling Method (NATM) for the modeling of grouted anchors used to strengthen the rock during tunnel advance. The formulation is applied to a 3D simulation of the stepwise excavation of the Bocac tunnel [18]. The aim of this numerical example is to investigate the effect of grouted anchors on the stiffening of the rock mass during the excavation process.

The model incorporates all relevant elements of primary and secondary support in hard rock tunneling and considers the staged excavation sequence. The rock mass, the shotcrete shell, the temporary bracing slab and the concrete lining are represented in the finite element model by 20-noded quadratic hexahedral elements. The rock bolts, the pipe roof and the wire ribs are modeled using the formulation developed for embedded piles as described in Section 3, using 2-node beam elements with 6 degrees of freedom per node. A large friction coefficient of $\mu = 0.9$ is assumed to account for the bond between installed primary support and the rock mass. For the modeling of the tips of the rock bolts the tip condition described in Subsection 3.1 is employed. For the modeling of the rock mass, a Drucker-Prager plasticity model is used. Shotcrete, concrete, rock bolts and pipe roof are modeled by linear elastic materials. The material parameters are summarized in Table 2.

Table 2: Material parameters used in the finite element model of the Bocac tunnel

Layer	γ [kN/m^3]	φ [°]	c [MPa]	E [MPa]	ν [-]
Lime 1 (1)	26.6	45.0	0.25	4300	0.26
Lime 2 (2)	26.8	57.0	0.9	11000	0.24
Lime 3 (3)	25.8	29.0	0.11	2100	0.28
Lime 4 (4)	26.0	48.0	0.4	4200	0.3
Clay (5)	21.0	18.0	0.05	400	0.38
Lime 5 (6)	25.8	25.0	0.2	1000	0.28
Steel bolts	76.2	-	-	210000	0.2
Concrete lining	25.0	-	-	30000	0.3

The discretized finite element model of the Bocac tunnel is shown in Figure 9. The staged excavation process is simulated by deactivating the

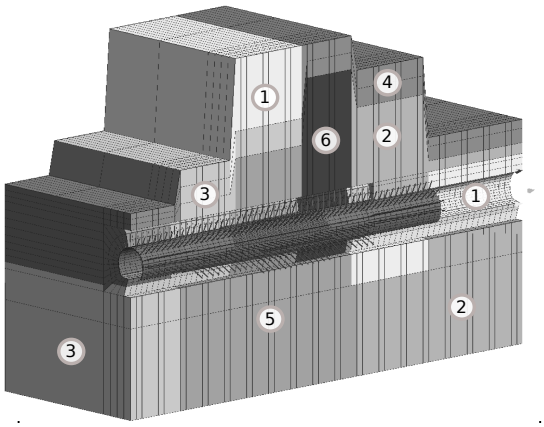

Figure 9: Finite element model of the Bocac tunnel (the differently shaded areas denote respective layers of different ground according to Table 2)

elements representing the excavated domain following the sequence of partial excavations of the crown, bench and the invert. The crown excavation is 16 m ahead of the bench excavation. After a section of two meters is excavated, the primary support, the shotcrete lining, the rock bolts and a temporary horizontal bracing slab are installed. The shotcrete lining is installed after the complete cross section of the tunnel is excavated. This is in agreement with the NATM principles, since the pressure from the rock mass is taken by the primary support. In order to evaluate the effect of the grouted anchors on the deformations during tunneling, a second simulation has been performed, with exactly the same geometry, support measures and model parameters as in the previous analysis, with the only difference that now no rock bolts were installed during the excavation process.

Figure 10 shows the total displacements of three points of the tunnel lining along a 32 m long tunnel section after installation of the primary support. The displacements are plotted for three points on the crown, the bench and the invert of the tunnel lining as shown in the illustration below the plots in Figure 10. The anchors significantly reduce the displacements of the tunnel lining at the crown and the bench of the tunnel. At the bottom of the tunnel, however, no anchors are installed. Thus, the comparison of the simulation with and without anchors does not exhibit differences in the invert area.

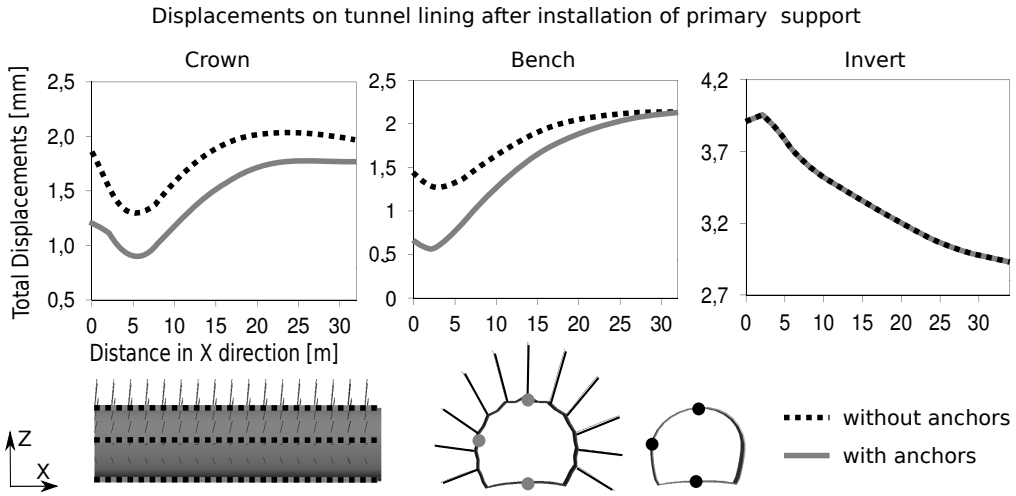

Figure 10: Effect of embedded rock-bolts on the stiffening of the rock mass during staged NATM tunneling process

4. Parallelization of the finite element model for mechanized tunneling

The parallelization concept investigated in this study encompasses three variants that are suitable for a variety of hardware configurations. On large multi-core shared memory systems, an openMP-based shared memory parallelization strategy is used that runs the most computationally expensive parts of the program in parallel. For computer clusters, a shared memory parallelization technique based on the Message Passing Interface (MPI) is applied. Here, a decomposition of the simulation model into small subdomains is used to distribute the workload on multiple computers.

The openMP-based shared memory parallelization is the most simple approach, since only little effort must be taken to manage memory access. However, a number of algorithmic measures have been implemented to increase the data throughput and to avoid communication bottlenecks for non-uniform memory access (NUMA) architectures. The two most time-consuming parts of a finite element simulation are the assembling of the system matrix and the solution of the system equations. Using openMP, sections of the code have been identified that can be performed in parallel. These sections can be marked with a special compiler directive and are automatically parallelized by a suitable compiler. Parallel regions in the pro-

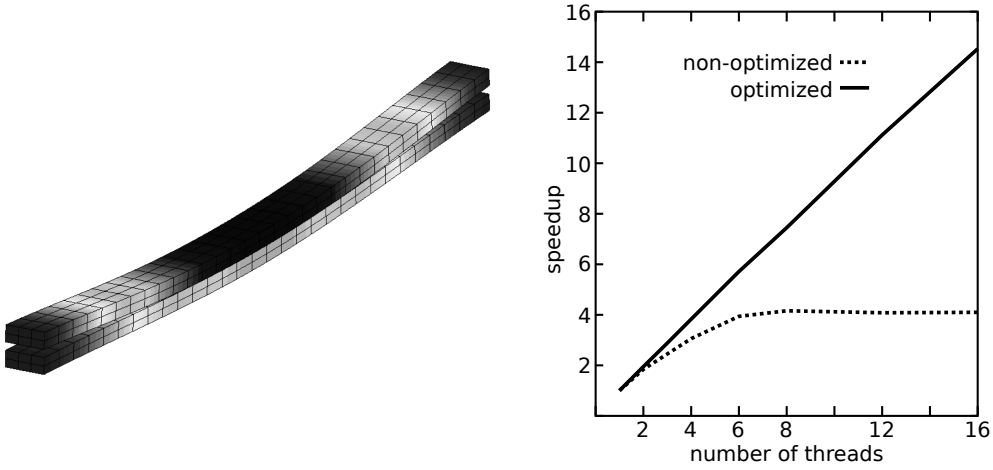

Figure 11: Effect of optimisations of memory allocation regarding non-uniform memory access on the assembling speedup

posed simulation model are the assembling of the system matrix, the linear solver and several smaller parts of the program as for example the transfer of variables from one mesh to another.

The assembling process is organized element-wise, that is the computation of each elemental contribution to the global system can be computed independently. The only possible conflict occurs at the writing access to the system matrix. Since this is fast in comparison to the elemental computations (e.g. of the constitutive law), it can be easily handled by means of locks. What is important, though, is the allocation of memory for the system matrix. If this is done solely in the local memory of one processor, all data access will be routed through this processor. In a hypercube architecture like applied in medium-sized multi-core computers with non-uniform memory access (NUMA), this means an over-utilisation of only one processor link while the rest of the cross-connections remain vastly idle. Hence, the memory is allocated piecewise distributed among all processors. Thus, the memory access pattern during the assembling process is arbitrarily distributed over all communication links.

To investigate the effect of these measures, a simple benchmark problem as shown in Fig. 11 has been investigated. It consists of two beams of different stiffness, the upper one being exposed to gravity load. The upper beam

bends down until it touches the lower beam which is then loaded by contact forces. The benchmark has been chosen because it involves a considerably large computational workload in the assembling process due to contact conditions and quadratic elements. The benchmark has been run using different numbers of threads on a 16-core Opteron machine. Figure 11 shows the effect of this optimized memory allocation. The right figure shows a plot of the speedup versus the number of threads. It can be seen that in the case of uniform allocation, the maximum speedup is limited to 4, after which the communication bandwidth is fully used. Using optimized memory allocation, the speedup is close to linear across all 16 threads.

In a distributed memory environment, domain decomposition methods are applied to distribute the computing of both the internal and external force vectors as well as the element and contact stiffness matrices across several computer nodes. In the proposed model, a non-overlapping domain decomposition is applied using a distributed data structure provided by the Trilinos project [30]. The main advantage of this data structure is that the distributed system matrices can be accessed throughout the model as a virtually monolithic data source. All MPI communication is encapsulated in the program kernel such that no particular measures must be applied to ensure that each element or constitutive law can be parallelized on distributed memory systems. In order to perform a spatial search for contact surfaces, a master and a slave surface is defined in the model. These surfaces are stored in a dedicated subdomain of the decomposed model (see Fig. 12).

As a consequence of the distributed data structure, the setup of the solution process is independent from the domain decomposition scheme used for the assembling. Hence, also the solution of the system equations can be performed in a distributed manner. Arbitrary distributed solvers can be employed, since the decomposition of the system equations is independent from the decomposition of the assembling process. In the simulation model for mechanized tunneling, the most important requirement for the solver is its capability to solve ill-conditioned, non-symmetric matrices that arise from the multi-phase soil model, the contact formulation and the nonlinear constitutive models. Since direct solvers are generally not efficiently parallelized, the use of iterative solvers has been a major goal in the development of the distributed memory version of the simulation model. Here, in particular the preconditioning of the coefficient matrix is of high importance since the conditioning affects not only the convergence speed but also the ability to find a solution by means of iterative solvers. The effectivity of a preconditioner

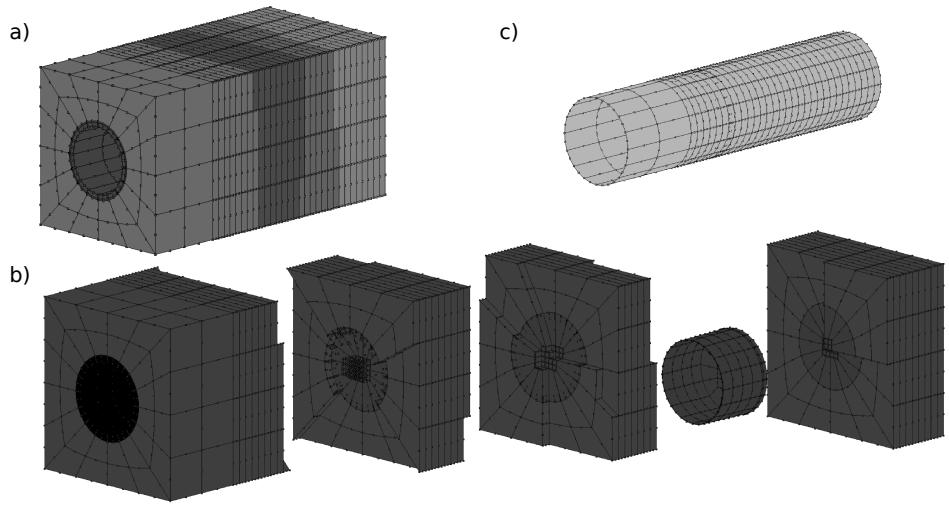

Figure 12: Domain decomposition considering the TBM-soil interface in the parallelized simulation model: a) decomposed model; b) subdomains of the model; c) dedicated domain for contact surfaces

strongly depends on the problem to be solved. For the proposed simulation model for mechanized tunneling, it has been found that a combination of a *KLU* preconditioner [31] and a *Generalized Minimal Residual solver* (GMRES) [32] yields reasonably good speedups (see Fig. 14b) compared to the assembling process (see Fig. 14a) [33]. The figures show the speedup of two different instances obtained from the simulation model in a benchmark test using two models with different numbers of DOFs (small model: 37,593 DOFs, large model: 148,857 DOFs) as shown in Fig. 13. From the comparisons in Figs. 14a and 14b it can be further concluded, that the size of the model has a large influence on the speedup performance. This is mainly due to the fact that for small system a decomposition causes more communication overhead than can be saved in terms of computation effort for the solution of each subdomain.

5. Concluding remarks

A simulation model for mechanized tunneling based on the finite element method has been successfully extended to represent the complete interaction mechanisms of the tunnel construction process with the surrounding soil and, in particular, with existing buildings on pile foundations. The sim-

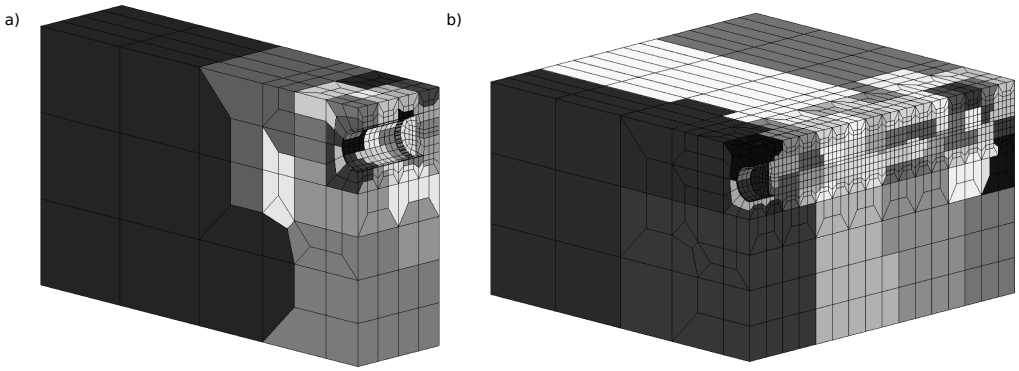

Figure 13: Distributed memory speedup test: a) small model; b) large model

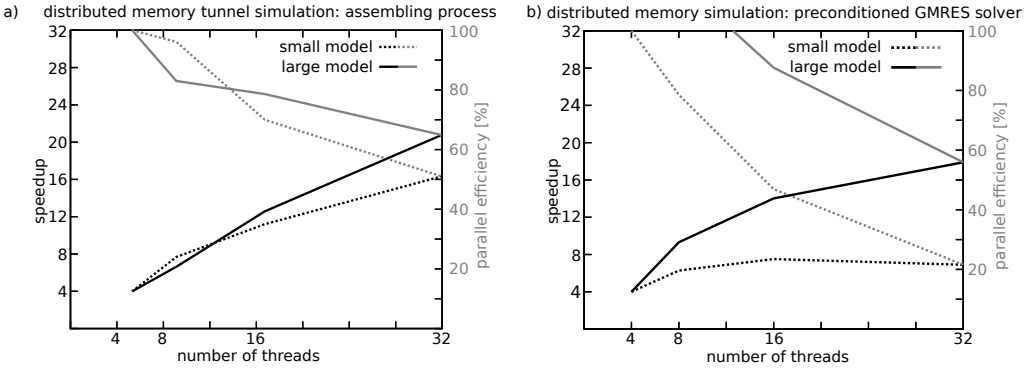

Figure 14: Speedup of small and large tunnel models: a) assembling process; b) iterative solving process

ulation model is able to capture all influences of the tunneling process on the surrounding ground and the built environment and can be employed as a platform for the investigation of all relevant interaction processes in urban tunneling in the design, but in particular also in the construction stage of tunneling projects. For the modeling of pile groups an embedded pile formulation allowing for consideration of arbitrary number of piles with arbitrary orientations independently from the spatial discretization of the soil has been proposed. Frictional contact along the height of the pile as well as the tip resistance has been considered. It was shown, that this model can be applied to the analysis of tunnel advance underneath existing buildings as well as for the modeling of grouted anchors and pipe roofs often used in tunneling as primary support after excavation. The applicability for these two cases has been demonstrated by two benchmark examples. This model was connected to a previously developed process-oriented simulation model for mechanized tunneling, which was also shortly described in the paper. In particular, parallelization strategies for both shared and distributed memory computers were presented that have been tailored to the particular requirements of the specific model developed for mechanized tunneling. From selected benchmark analyses it is concluded, that for distributed computing using domain decomposition methods the GMRES solver in conjunction with a KLU preconditioner provides best performance among the investigated variants. Currently, further research is conducted to improve the effectivity and efficiency of the preconditioning in distributed memory architectures account for the specific properties of matrices involved in the presented model for mechanized tunneling.

6. Acknowledgements

Financial support was provided by the German Science Foundation (DFG) in the framework of project C1 of the Collaborative Research Center SFB 837. The work of the second author was also supported by the Ruhr-University Research School funded by Germany's Excellence Initiative (DFG GSC 98/1). This support is gratefully acknowledged.

[1] G. Beer (Ed.), Numerical Simulation in Tunnelling, Springer, Wien - New York, 2003.

[2] S. Bernat, B. Cambou, Soil - structure interaction in shield tunnelling in soft soil, Computers and Geotechnics 22 (3/4) (1998) 221–242.

[3] K. Komiya, K. Soga, H. Akagi, T. Hagiwara, M. Bolton, Finite element modelling of excavation and advancement processes of a shield tunnelling machine, Soils and Foundations 39 (3) (1999) 37–52.

[4] D. Dias, R. Kastner, M. Maghazi, Three dimensional simulation of slurry shield tunnelling, in: O. Kusakabe, K. Fujita, Y. Miyazaki (Eds.), Geotechnical Aspects of Underground Construction in Soft Ground, Tokyo 1999, Balkema, Rotterdam, 2000, pp. 351–356.

[5] G. Swoboda, Abu-Krisha, Three-dimensional numerical modelling for tbm tunnelling in consolidated clay, Tunnelling and Underground Space Technology 14 (1999) 327–333.

[6] T. Kasper, G. Meschke, A 3D finite element model for TBM tunneling in soft ground, International Journal for Numerical and Analytical Methods in Geomechanics 28 (2004) 1441–1460.

[7] T. Kasper, G. Meschke, On the influence of face pressure, grouting pressure and TBM design in soft ground tunnelling, Tunnelling and Underground Space Technology 21 (2) (2006) 160–171.

[8] F. Nagel, J. Stascheit, G. Meschke, A. Gens, T. Rodic, Process-oriented numerical simulation of mechanised tunnelling, in: G. Beer (Ed.), Technology Innovations in Underground Construction, Taylor and Francis, 2009, pp. 87–127.

[9] J. Stascheit, F. Nagel, G. Meschke, M. Stavropoulou, G. Exadaktylos, An automatic modeller for finite element simulations of shield tunnelling, in: J. Eberhardsteiner, G. Beer, C. Hellmich, H. Mang, G. Meschke, W. Schubert (Eds.), Computational Modelling in Tunnelling (EURO:TUN 2007), Vienna, Austria, 2007, CD-ROM.

[10] H. Yu, CASM: a unified state parameter model for clay and sand, International Journal for Numerical and Analytical Methods in Geomechanics 48 (1998) 773–778.

[11] F. Nagel, G. Meschke, An elasto-plastic three phase model for partially saturated soil for the finite element simulation of compressed air support in tunnelling, International Journal for Numerical and Analytical Methods in Geomechanics 34 (2010) 605–625. doi:10.1002/nag.828.

[12] C. Desai, G. Appel, 3-d analysis of laterally loaded structures, in: Proceedings 2nd International Conference On Numerical Methods in Geomechanics, Vol. 1, ASCE, Blacksburg, 1976, pp. 405–418.

[13] Z. Yang, B. Jeremić, Numerical analysis of pile behavior under lateral loads in layered elastic-plastic soils, International Journal for Numerical and Analytical Methods in Geomechanics 26 (14) (2002) 1385–1406.

[14] Z. Yang, B. Jeremić, Study of soil layering effects on lateral loading behavior of piles, Journal of Geotechnical and Geoenvironmental Engineering 131 (6) (2005) 762–770.

[15] L. F. Miao, A. T. C. Goh2, K. S. Wong, C. I. Teh, Three-dimensional finite element analyses of passive pile behaviour, International Journal for Numerical and Analytical Methods in Geomechanics 30 (7) (2007) 599–613.

[16] K. A. Petek, Development and application of mixed beam-solid models for analysis of soil-pile interaction problems, Ph.D. thesis, University of Washington (2006).

[17] M. Sadek, I. Shahrour, A three dimensional embedded beam element for reinforced geomaterials, International Journal for Numerical and Analytical Methods in Geomechanics 28 (2004) 931–946.

[18] J. Ninić, J. Stascheit, G. Meschke, D. Divac, Numerical simulation of natm tunnel construction for the bocac tunnel project –a comparison of 2d and 3d analyses, in: 1st International Congress on Tunnels andUunderground Structures in South-East Europe - Using Underground Space, Croatian Association for Tunnelling and Underground Structures, ITA Croatia, Dubrovnik, Croatia, 2011, pp. 1–10, published on USB Stick.

[19] J. Stascheit, M. Eitzen, G. Meschke, Parallel simulation of shield tunnelling on distributed memory and gpgpu systems, in: P. Ivanyi, B. H. V. Topping (Eds.), Proceedings of the Second International Conference on Parallel, Distributed, Grid and Cloud Computing for Engineering, Civil-Comp Press, Stirlingshire, UK,, Ajaccio, France, 2011, CD-ROM, Paper 28, 2011. doi:10.4203/ccp.95.28.

[20] G. Meschke, F. Nagel, J. Stascheit, Computational simulation of mechanized tunneling as part of an integrated decision support platform,

Journal of Geomechanics (ASCE)Published online since May 2010. doi:http://dx.doi.org/10.1061/(ASCE)GM.1943-5622.0000044.

[21] F. Nagel, J. Stascheit, G. Meschke, A simulation model for shield tunnelling and its interactions with partially saturated soil, Proceedings of Applied Mathematics and Mechanics 9 (1) (2009) 215–216.

[22] P. Dadvand, R. Rossi, E. Oñate, An object-oriented environment for developing finite element codes for multi-disciplinary applications, Archives of Computational Methods in Engineering 17 (2010) 253–297.

[23] F. Nagel, G. Meschke, Three-phase modeling in partially saturated soils, Proceedings in Applied Mathematics and Mechanics 7 (1) (2007) 4070009–4070010.

[24] C. Blom, Design philosophy of concrete linings for tunnels in soft soils, Ph.D. thesis, Delft University (2002).

[25] F. Nagel, J. Stascheit, G. Meschke, A simulation model for shield tunnelling with compressed air, Geomechanics and Tunneling 1 (3) (2008) 222–228.

[26] F. Nagel, G. Meschke, Grout and bentonite flow around a TBM: Numerical simulations addressing its impact on surface settlements, Tunnelling and Underground Space Technology incorporating Trenchless Technology Research 26 (2011) 445–452.

[27] P. Wriggers, T. Van, E. Stein, Finite element formulation of large deformation impact-contact problems with friction, Computers & Structures 37 (3) (1990) 319–331.

[28] T. Laursen, Computational Contact and Impact Mechanics, Springer, Berlin-Heidelberg, 2002.

[29] P. Wriggers, Nonlinear Finite Element Methods, Springer-Verlag Berlin Heidelberg, 2008.

[30] M. A. Heroux, R. A. Bartlett, V. E. Howle, R. J. Hoekstra, J. J. Hu, T. G. Kolda, R. B. Lehoucq, K. R. Long, R. P. Pawlowski, E. T. Phipps, A. G. Salinger, H. K. Thornquist, R. S. Tuminaro, J. M. Willenbring, A. Williams, K. S. Stanley, An overview of the trilinos project, ACM Trans. Math. Softw. 31 (3) (2005) 397–423.

[31] E. P. Natarajan, Klu - a high performance sparse linear solver for circuit simulation problems, Master's thesis, University of Florida (2005).

[32] Y. Saad, M. Schultz, Gmres: A generalized minimal residual algorithm for solving nonsymmetric linear systems, SIAM J. Sci. Stat. Comp. 7 (1986) 856–869.

[33] J. Stascheit, Parallelisation and model generation methods for large-scale simulations of shield tunnelling processes, Ph.D. thesis, Ruhr-Universität Bochum (2010).